Supplemental

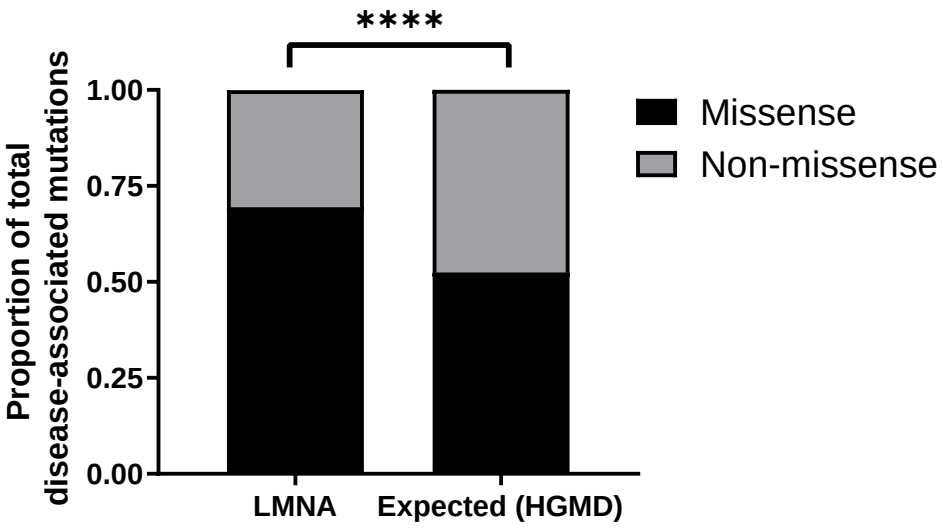

Supplemental Figure 1. Proportion of missense mutations in *LMNA* versus all known disease-associated mutations (Human Gene Mutation Database). *LMNA* vs. expected: Fisher's exact test, p<0.0001.

Phenotype		Geographic Origin					
		Europe	Africa	Americas	Oceania	Asia	Unknown
Striated	Myopathy	17 (35%)	-	7 (15%)	3 (6%)	16 (33%)	5 (10%)
	Cardiomyopathy	282 (56%)	5 (1%)	78 (16%)	-	73 (15%)	62 (12%)
	Both	254 (53%)	2 (<1%)	55 (12%)	-	61 (13%)	105 (22%)
	Total	552 (54%)	7 (1%)	140 (14%)	3 (<1%)	150 (15%)	172 (17%)
Lipodystrophy/Metabolic		76 (24%)	-	16 (5%)	-	20 (6%)	203 (64%)
Neuropathy		-	44 (96%)	1 (2%)	-	-	1 (2%)
Progeria		22 (18%)	3 (2%)	31 (25%)	-	13 (11%)	54 (44%)
Bone/Skin		14 (44%)	3 (9%)	4 (13%)	-	8 (25%)	3 (9%)
Overlap		56 (72%)	2 (3%)	13 (17%)	1 (1%)	3 (4%)	3 (4%)
Total		**721 (45%)**	**59 (4%)**	**205 (13%)**	**4 (<1%)**	**194 (12%)**	**436 (27%)**

Supplemental Table 2. Reported patient geographic origin by phenotype.

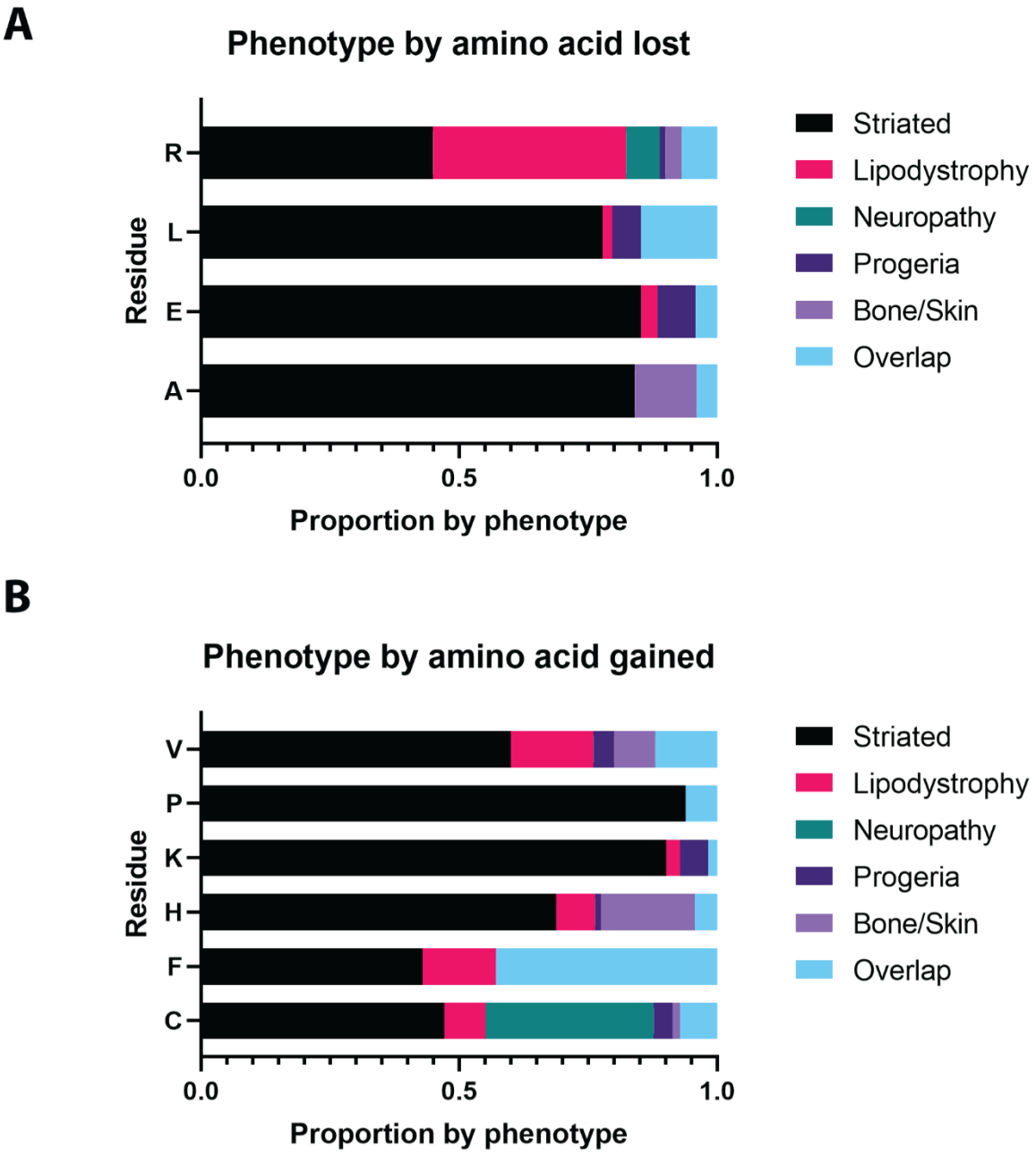

Supplemental Figure 2. Phenotype sorted by amino acid change. A) Phenotype by amino acid lost: the most commonly gained amino acid residues as a result of missense mutations charted by the phenotype observed. B) Phenotype by amino acid lost: the most commonly lost amino acid residues as a result of missense mutations charted by the phenotype observed.

Phosphorylation change	Mutation	Possible P-site	Possible Kinase (family)
Gain	L52P	51	CDK, MAPK
	A278P	277	CDK, MAPK
	L302P	301	CDK, MAPK
	Q396R	398	PKA
	T528R	533	(Akt)
	G635D	(632, 652)	CK2
Loss	P4R	3	MAPK, CDK
	T10I	10	PKA, PKC
	S22L	22	CDK, MAPK
	R48P	51	PKC
	S277P	277	PKA, PKC
	R298C	301	PKC
	R388C	390	PKA
	R388H	390	PKA
	S395L	395	PKC
	R401C	403, 404	PKA, PKC
	R427G	429	PKA
	D461Y	458	CK2
	R455P	458	PKC
	R482L	480	PKC
	R482Q	480	PKC
	R482W	480	PKC
	R541C	546	(Akt)
	R545C	548	(CHEK1/2, Akt)
	R527C	(525, 533, 534)	PKC
	R527H	(525, 533, 534)	PKC
	R527L	(525, 533, 534)	PKC
	R527P	(525, 533, 534)	PKC

Supplemental Table 3. A list of putative kinase P-sites that were predicted to be gained or lost by both computational tools, sorted by phosphorylation site.

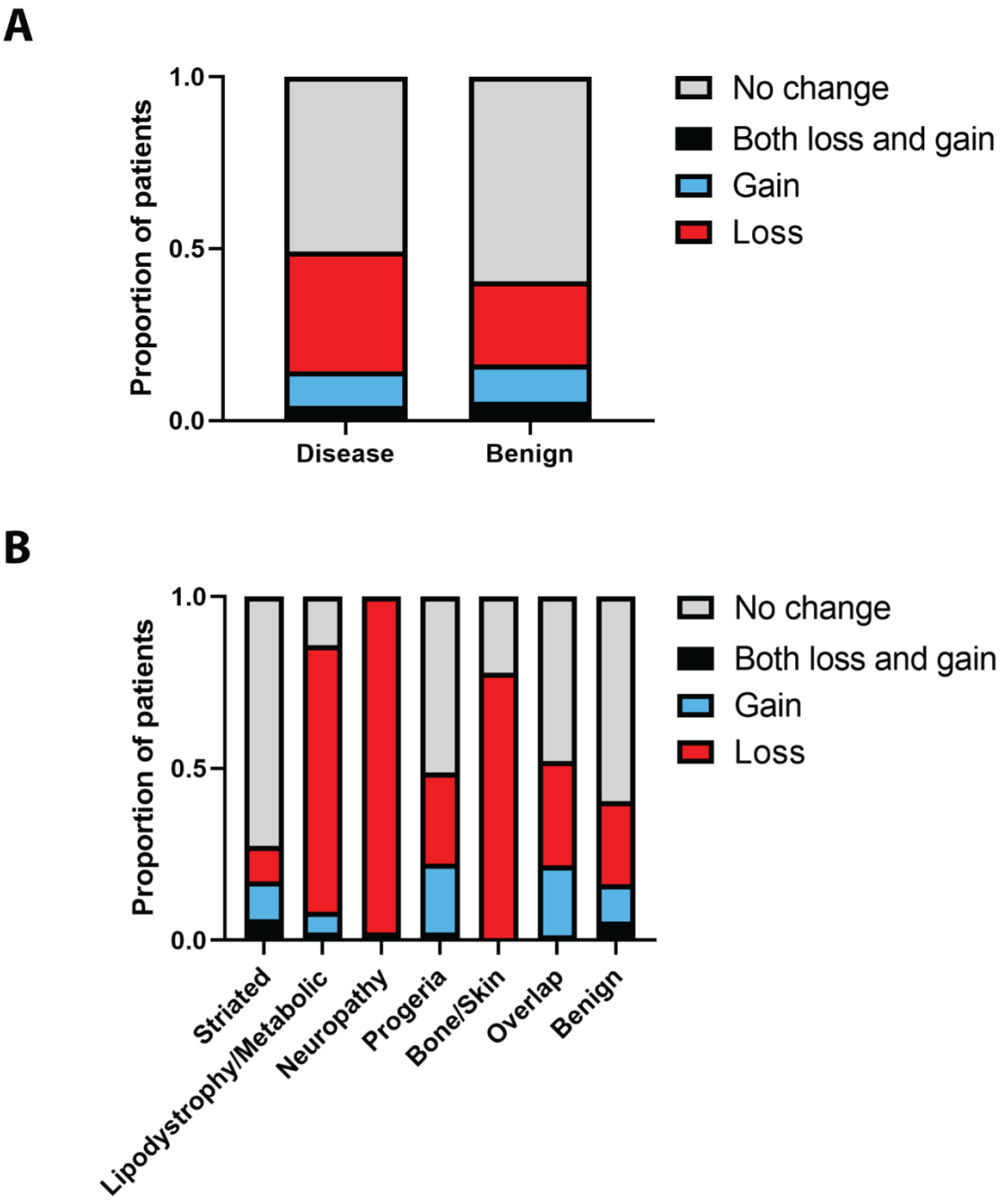

Supplemental Figure 3. Predicted phosphorylation changes by disease status and phenotype. A) Predicted phosphorylation in disease vs. benign groups: the proportion of patients with variants associated with disease or not predicted to result in loss, gain, both, or no change in phosphorylation. B) Predicted phosphorylation changes by phenotype: the proportion of patients by phenotype with variants predicted to result in loss, gain, both, or no change in phosphorylation.

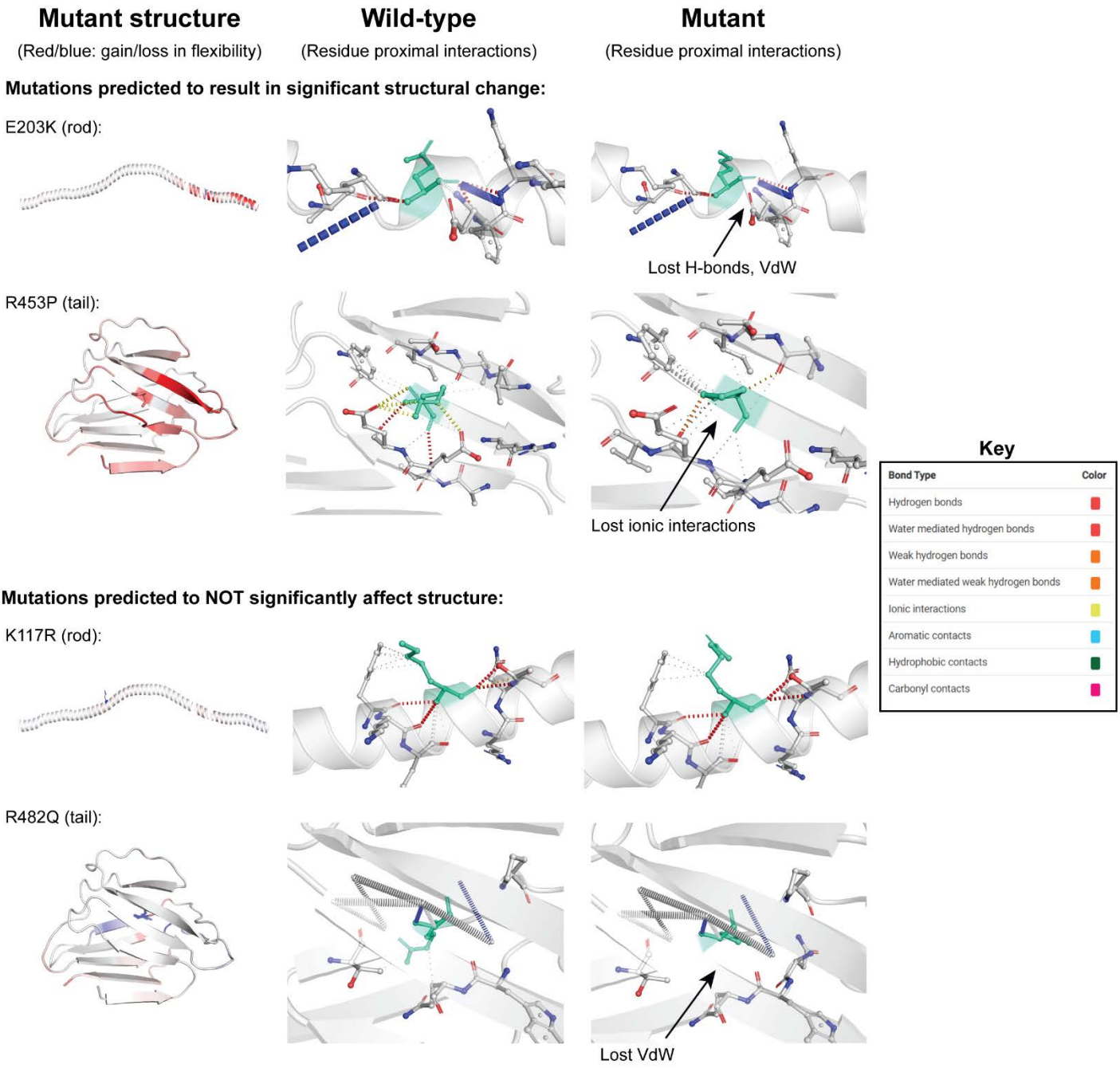

Supplemental Figure 4. Example verification of predicted structural changes. Modeling of point mutations and visualization performed using DynaMut (see Methods). Depicted are two example hotspot missense mutations from both rod (PDB: 6JLB chain A, residues 46-247) and tail (PDB: 1IFR, residues 432-544) domains, either predicted to undergo significant structural change or be structurally preserved. From left to right: 1) global structure depicted in the form of coiled domain or globular domain, with red indicated increased flexibility in the protein induced by the mutation; 2) Cartoon of wild-type residue (in mint green) and neighboring interactions, color coded based on key; 3) Cartoon of mutant residue (in mint green) and neighboring interactions, with lost interactions from mutations labeled by arrow(s). Interactions are largely preserved in the bottom half panel, with only relatively minor interactions lost, if any. VdW, Van der Waals.

Supplemental Table 1. Compiled mutational (cDNA variant, amino acid change, exon, domain, mutation type) and clinical data (phenotype, heterozygosity status, sex, and geographic origin) from all sources in this study (Human Intermediate Filament Database, Universal Mutation Database, UniProt, and literature review), comprising 1890 individuals and 404 unique mutations. Possible post-translational modification associated with each residue, according to UniProt, are also included.